Effects of process parameters on structure and corrosion behavior of PEO coated A356 alloy

Article *in* Surface Topography Metrology and Properties · November 2020

DOI: 10.1088/2051-672X/abc736

3 authors, including:

Sina Rahimi
Materials and Energy Research Center
5 PUBLICATIONS **23** CITATIONS

SEE PROFILE

Surface Topography: Metrology and Properties

PAPER

RECEIVED
19 August 2020

REVISED
20 October 2020

ACCEPTED FOR PUBLICATION
3 November 2020

PUBLISHED
10 November 2020

Effects of process parameters on structure and corrosion behavior of PEO coated A356 alloy

Sina Rahimi*, Benyamin Yarmand* and Alireza Kolahi

Nanotechnology and Advanced Materials Department, Materials and Energy Research Center (MERC), Karaj, Iran

* Authors to whom any correspondence should be addressed.

E-mail: s.rahimi@merc.ac.ir **and** byarmand@merc.ac.ir

Keywords: Plasma electrolytic oxidation (PEO), A356 aluminum alloy, process parameters, microstructure, corrosion

Abstract

Plasma electrolytic oxidation (PEO) coatings were formed on cast A356 aluminum alloy by applying various process parameters (current density, duty cycle and processing time) in silicate based electrolyte. The phase composition of coatings was analyzed by x-ray diffraction (XRD), surface and cross section morphology and microstructure of coatings were characterized by scanning electron microscope (SEM). The Results of x-ray diffraction showed that all coatings are composed of gamma alumina. Coating produced in higher current density, duty cycle and time was more compact with fewer amounts of defects. Thickness and roughness of coatings surfaces were measured by Eddy current gauge and surface roughness tester, respectively. The thickness of the Coatings was in the range of 3–7 μm and it increased by increasing current density and time, but duty cycle did not have a noticeable effect on it. Corrosion resistance of bare and coated samples was evaluated by polarization test in 3.5 wt% NaCl solution. Sample S176 showed the best corrosion resistance with corrosion current density of 4.17×10^{-8} A.cm^{-2} and polarization resistance of 6.31×10^{5} Ω.cm^{2} that attributed to its more dense structure.

Introduction

Among the aluminum alloys, cast aluminum-silicon alloys are popular for their variety of applications in automotive industries owing to their excellent castability and thermal conductivity as well as good mechanical properties. However, their weak corrosion resistance in severe corrosive environments limited their applications [1, 2]. Anodic oxidation or anodizing process is a common coating method for producing protective layer on cast aluminum-silicon alloys. But, this layer could not provide sufficient wear and corrosion properties because of its porous structure and brittleness. Moreover, presence of silicon phases prevents the formation of a thick and uniform coating on these alloys by anodizing process [3–5].

Plasma electrolytic oxidation (PEO) or micro arc oxidation is a newly developed method for fabrication of protective oxide layers on aluminum, titanium and magnesium and their alloys. PEO is derived from anodizing but the applying potential range is higher than faraday region and it causes micro-arc discharges [6–8]. As a result of the occurrence of micro-arc discharge, the oxide layer on the sample surface was melted locally and it solidified again in contact with cool surrounding electrolyte. The result of the recurring process of melting and solidifying of the oxide layer is the disintegration of the initial ordered oxide layer and the formation of secondary dense and porous layers.

The characteristics of the coating formed by PEO process are influenced by several parameters including current density, duty cycle, oxidation time, electrolyte chemical composition, type and amount of the electrolyte additives, chemical composition and microstructure of substrate [9, 10].

Thus far, limited research has been done to achieve optimum conditions of process parameters for the production of PEO coating on cast aluminum-silicon alloys. Nie *et al* [11] investigated the effect of substrate Si content on the PEO coating formation, composition and morphology and they found that coating formation had four stages, at all stages coating on Si rich regions was more porous than coating on aluminum rich regions and higher content of Si resulted in rougher coating surface. Xia *et al* [12] produced PEO

coatings on aluminum-silicon alloy containing bulk primary Si under different treatment times to study effect of these bulk primary Si on the coating properties. They reported that in short times and early stages of oxidation, the coating on these particles was rougher than the coating on aluminum-silicon alloy with eutectic composition. Also, they understood that a long time is needed to form a uniform oxide layer on the substrate, which is a function of bulk primary silicon size. In another research, Cheng *et al* [13] studied the effect of sodium aluminate concentration on the corrosion and wear properties of PEO coating on A356 aluminum alloy. They concluded that coating formed in 24 g l^{-1} sodium aluminate had the best corrosion and wear resistance because of its compact and almost single layer structure.

It is well known that electrical parameters and time have a very important effect on the coating formation mechanism during electrochemical processes, hence, many researchers have investigated the effect of these parameters on the different properties of PEO treated aluminum alloys; however, the majority of these studies have been devoted to wrought alloys [14–19], while to the knowledge of the present authors, the effect of abovementioned parameters on microstructural and corrosion properties of the PEO treated cast aluminum-silicon alloys, has not been investigated yet. Therefore, in the present study, effect of current density, duty cycle and oxidation time on the thickness, roughness, phase formation, microstructure and corrosion resistance of the PEO coatings on cast A356 aluminum alloy were investigated.

Materials and methods

Rectangular samples (2 cm × 1 cm × 0.5 cm) of cast A356 aluminum alloys (6.5–7.5 Si, 0.12 Fe, 0.10 Cu, 0.30–0.45 Mg, 0.05 Mn, 0.05 Zn, 0.20 Ti, the balance Al) were used as substrate for coating deposition. Samples were polished with SiC abrasive paper up to 2000 grit in order to reach a surface roughness (R_a) of 0.1 μm, then degreased in ethanol using ultrasound and finally dried in warm air. An electrolyte was made from a aqueous alkaline solution of sodium silicate (10 g l^{-1}) and KOH (2 g l^{-1}) in deionized water. Surface oxidation process was done by pulsed direct current power supply with 1000 Hz modulation. The prepared sample was connected to the positive pole (anode) and the negative pole of the power source connected to the stainless steel cathode with water-circulator system. The electrolyte temperature remained about 25 °C during the PEO process. In order to evaluate the effect of current density, duty cycle and oxidation time on properties of resulted coating, different combination of these parameters were used for coating process, which are presented in table 1. PEO was conducted in constant current density mode and the current density values which are given in table 1 are average values.

Table 1. Different parameters used for coating process.

Sample	Current density (A cm^{-2})	Duty cycle (%)	Time (min)
S576	0.05	75	60
S176	0.11	75	60
S171	0.11	75	15
S156	0.11	50	60

Thickness and roughness (R_a) of coatings were measured using an Eddy current gauge (Phynix-FN) and portable surface roughness tester (TR100), respectively. X-ray diffraction (XRD, Philips) with CuKα radiation, 40 kV, 35 mA and 0.02_/s scan rate were used to study the phase composition of PEO coatings. The microstructural features and elemental composition of the specimens were analyzed using a scanning electron microscope (SEM, TESCAN MIRA3) equipped with an energy dispersive X-ray spectrometer (EDS). The average value of coatings surface porosities was estimated by image analysis using image j software. Corrosion properties of samples were assessed by potentiodynamic polarization method using potentiostat (EG & G) equipment. A three-electrode cell containing bare and coated samples as anode, a platinum wire as auxiliary electrode and a saturated calomel electrode as reference were used. All specimens were evaluated at 25 °C in a 3.5 wt% NaCl solution with effective surface area of 1 cm^2. Samples were placed in solution for 6 h before the test to reach the potential of open circuit potential. The potentiodynamic Polarization tests were performed at a potential range of −1500 mV to 250 mV and with a scan rate of 1 mV s^{-1}.

Results and discussions

During the PEO process of A356 aluminum alloy, the voltage-time response (V–T) of samples was recorded. Figure 1 shows the V–T curves of S576, S176 and S156 samples. All of the V–T curves can be divided into four stages. The first stage shows anodic oxidation and the next three stages show PEO. The mechanism of oxide layer growth during the PEO coating formation has been reported elsewhere [11]. From figure 1, it can be found that the changes in electrical parameters had an intense effect on V–T curves. Also, the values of V_b and V_f as well as their alteration can be seen on V–T curves inside figure 1. In the first stage, a rapid linear increase of the voltage with process time can be observed and sparks were not still visible on the samples surface. At the end of this stage voltage reached to V_b value, which is related to the dielectric breakdown of the oxide layer. In the second stage, after breakdown voltage, voltage grew gradually, but rate of voltage changes decreased, and quite a few minute sparks is appeared

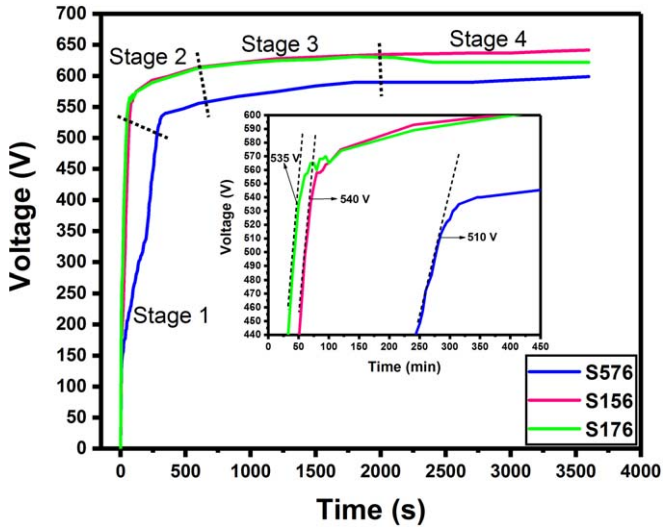

Figure 1. Voltage-time response of S576, S176 and S156 samples.

on the whole A356 aluminum alloy surface. These sparks likely prevent the uniform thickening of the barrier film, thus decreasing its rate of growth. Comparison of V–T curves indicates that the cell voltage increased in a shorter time for coating treated at higher current density. Accordingly, higher V_b were achieved for S176 sample than S576 sample. This change in V_b by increasing applied current density reveals that PEO process can be affected by current density which in turn can make alterations to the coatings growth and properties. Comparison of three V–T curves shows that the transformation of PEO process into stage two occurred faster in S156 and S176 samples which were treated in higher current density rather than S576 sample. Turning into stage three also happened faster in higher current density. According to the model suggested by Ikonopisov [14], when the cell voltage rises to a high enough value, dielectric breakdown will be occurred. This critical voltage is reached faster in higher current density. Therefore, micro discharges formed earlier and developed quicker. In other words, with increasing current density, PEO coating process commences in a shorter time which also is the reason for the earlier transformation to the next stages. From V_b values it can be found that a little lower voltage is required for the breakdown of the oxide layer of sample treated at higher duty cycle (S176), however, the difference was negligible. This tendency may be due to shorter on-time duration which requires more time to achieve breakdown voltage with lower duty cycle, whereas longer on-time duration may allow sufficient time to reach breakdown voltage with higher duty ratio. By progress in PEO process, the rate of voltage variation has decreased and four separated stages with different slope have distinguished on V–T curves. The V–T curve of S176 sample could show V–T responses of both S171 and S176 samples, because the time was only different process parameter for them. According to this curve, it can be seen that PEO process for S171 sample entered the stage three, while in S176 sample; PEO process passed stage three and went in stage four. By entering stage 4 in S176 sample, voltage decreased slightly and then stayed almost constant until the end of the process. This could be because chemical dissolution has overtaken the PEO coating process.

Figure 2 shows microdischarges images on the surface of the specimens at the end of the oxidation process. In figures 2(a) and (b), which are related to the S576 and S156 samples, respectively; the applied current density has increased from 0.05 A cm^{-2} to 0.11 A cm^{-2}. Comparison of microdischarges images showed that by increasing the current density, the intensity of microdischarges has increased, which can be due to an increase in the energy of each pulse [17]. Decreasing the duty cycle from 75% to 50% under constant current density and process time increased the number of microdischarges, but decreased their size and intensity, which can be obtained from the comparison of figures 2(b) and (d). The number of microdischarges decreased with extended PEO time, however size and intensity of them has increased. This increment of size and intensity of the microdischarges by increasing treatment time could be attributed to the decrement in the number of discharging areas. In other words, coating treated for longer time became thicker and had fewer numbers of weak areas for passing current and generating microdischarges. Therefore, more amount of current passed through these weak areas and caused bigger and stronger microdischarges to be appeared.

The average thickness changes of the oxide layer formed on the specimens under different conditions of the current density, duty cycle, and oxidation time are shown in figure 3(a). As it can be seen, coatings thicknesses were between 3 and 7.9 μm and were comparable to the literature [15, 20]. The average thickness

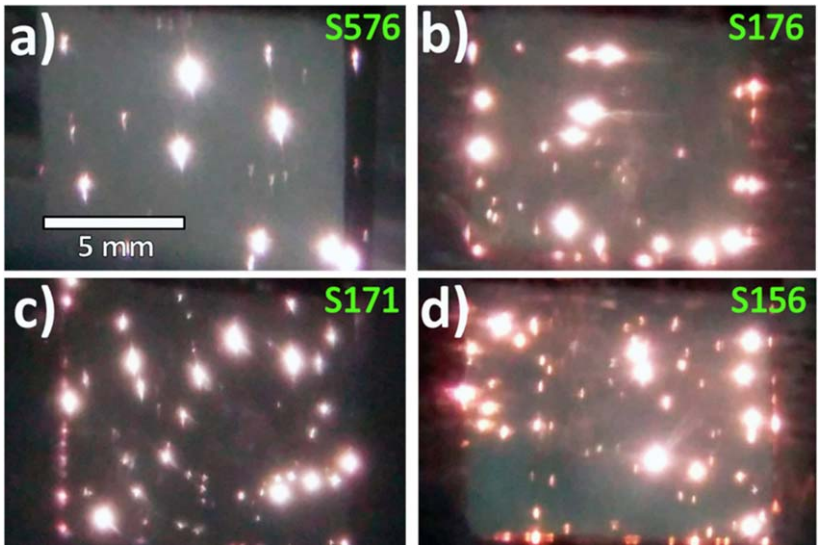

Figure 2. Microdischarges images on the surface of the samples at the end of process.

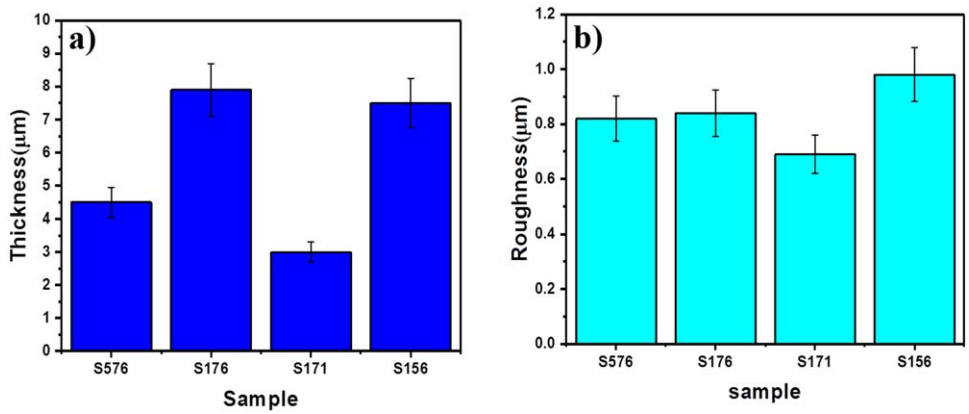

Figure 3. Results of (a) thickness and (b) roughness measurements.

of the oxide layer increased with increasing the current density and the oxidation time, but the change in duty cycle did not have a significant effect on the average thickness of the oxide layer, because the changes in duty cycle does not affect the number of cycles and the amount of energy per cycle is also constant, in other words, the increment in duty cycle neither influence the intensity of microdischarges, nor influence number of them. Hence, the thickness of the coating did not change considerably. Enhancement of the thickness of the coating by increasing the current density is related to the increased energy of the microdischarges. The oxide layer forms due to the ejection of molten materials from the discharge channels and their subsequent freezing after contact with the electrolyte [15]. Therefore, as the current density increases, the amount of energy of each microdischarge increases, causing more heat in the coating-substrate interface and wall of the discharge channels, so more of the substrate melts, oxidizes and makes coating. Also, time had a significant effect on PEO coating thickness and coatings produced in longer treatment time showed higher thickness which has been reported by many researchers in PEO coating of aluminum alloys [15, 21, 22].

Figure 3(b) shows the average surface roughness of the coatings (Ra (μm)) formed on the specimens under different conditions of the current density, duty cycle, and oxidation time. With increasing current density and oxidation time, the surface roughness increased which can be due to an increase in the coating thickness, because in coatings with higher thickness, it is more difficult for current to pass through coating and it is only able to pass through weak areas. Moreover, localizing of the anodic current in weak areas produced more powerful microdischarges which in turn increased the diameter of the discharge channels and caused higher surface roughness. Applying higher duty cycle reduced the roughness value of the coating surface. Such behavior of surface roughness in S176 sample compared to S156 sample could be related to its surface morphology, because the big pores

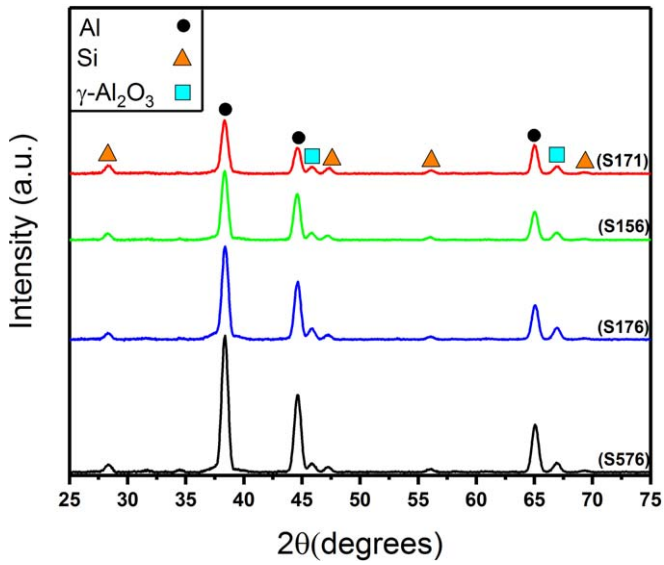

Figure 4. XRD patterns of coated samples.

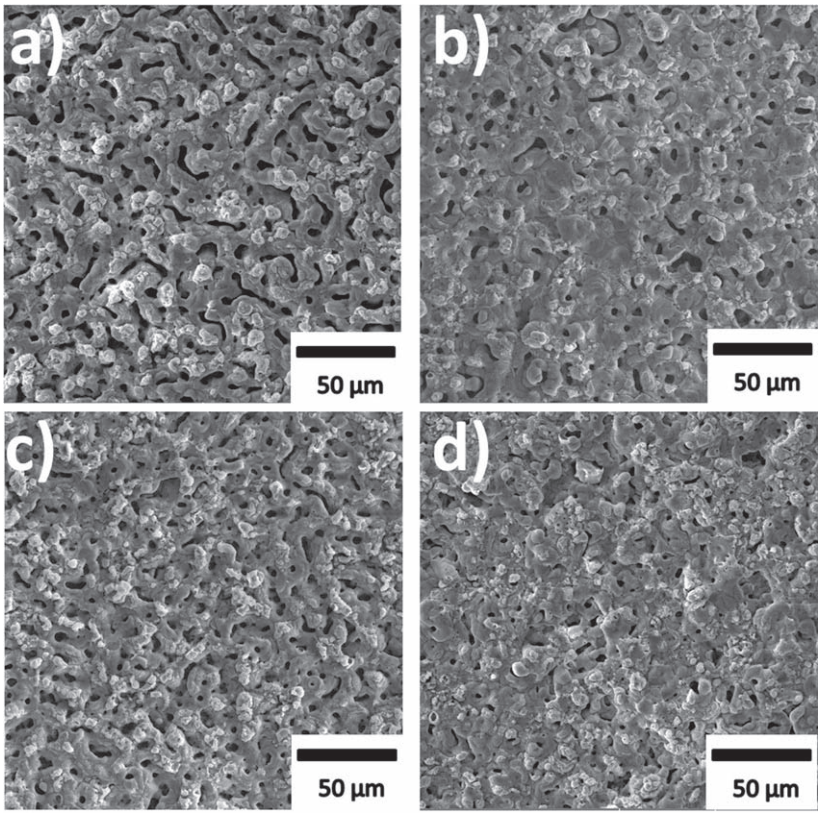

Figure 5. SEM images of PEO coating on (a) S576, (b) S176, (c) S171 and (d) S156 samples (1000×).

are joined together and number of them is decreased (figures 5 and 6).

Figure 4 Shows the x-ray diffraction spectra of S576, S176, S171 and S156 samples. The XRD patterns of all coated samples shows presence of γ-alumina phase Along with aluminum and silicon phases resulting from the substrate. In previous investigations [23, 24], it has been reported that aluminum substrate was melted by the heat of microdischarges, then transferred through discharges channels to the electrolyte and combined with the oxygen present in the electrolyte and after rapid freezing, provides the formation of the gamma phase. From patterns it can be deduced that coatings phase composition have not changed notably with duty cycle. On the other hand, with increasing current density and processing time, peaks

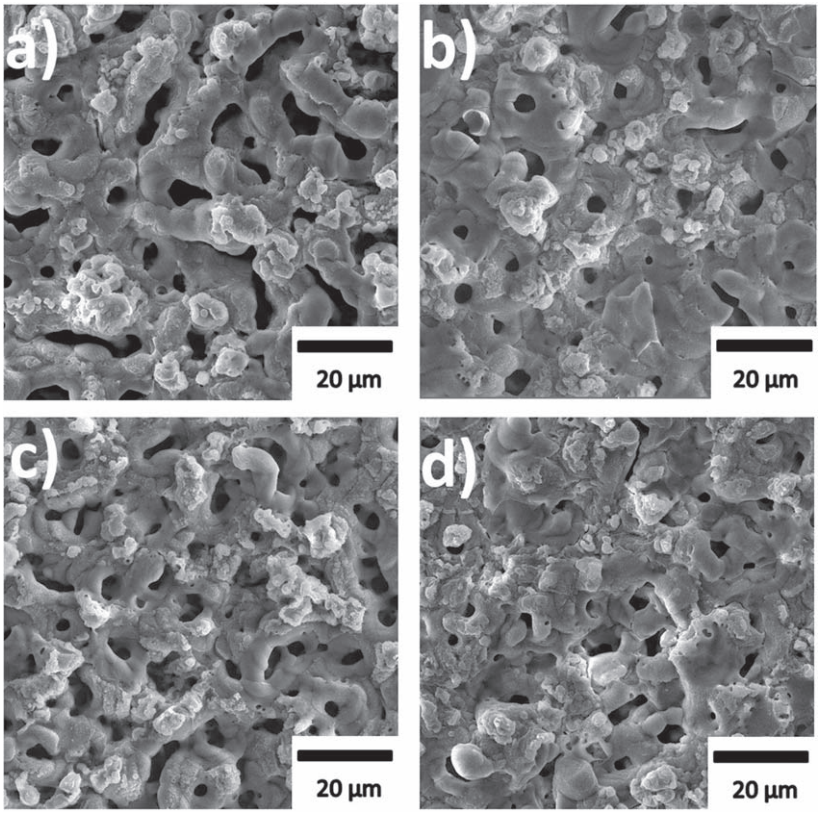

Figure 6. SEM images of PEO coating on (a) S576, (b) S176, (c) S171 and (d) S156 samples (2500×).

of γ-alumina in sample S176 showed a little higher intensity compared to S576 and S171 samples which could be attributed to its higher thickness. In addition, surface porosity percent is higher in S576 and S171 samples as compared to S176 that could affect X-ray reflectance from coating and decrease it.

Figures 5 and 6 show SEM images of surface morphology of the S576, S176, S171 and S156 samples in different magnifications. Process parameters, namely Current density, duty cycle, and oxidation time could make considerable changes to micro-discharges features. Accordingly, various kinds of coating morphology could be achieved in this study. The SEM images of the S576 and S171 shows that their surfaces contain many pores and the SEM images of the S176 and S156 samples indicate the presences of crater-like structures above them. In fact, central holes of the crater-like structures are discharge channels which are the ways for molten materials to be ejected and solidified on the surface. In the case of S176 Sample, majority of these discharge channels are filled with ejected materials. The surface composition of S576 sample by EDS is reported in figure 7. As shown in figure 7(a), composition of three different points on the coating surface was analyzed. The EDS analysis results reveal that the Al, O and Si are major elements in the coating. According to the elemental analysis of point A, which shows a high percentage of Al and O elements, it can be understood that the aluminum oxide has formed at this point. But at the points B and C, all three elements of Al, O and Si exist which shows these bright white areas are formed from alumina silicate phases As mentioned elsewhere [25]. Oxide products, including alumina and silicon dioxide are sources of element O, element Al originated from the substrate and element Si may be come to the coating either from the substrate or from SiO_3^{2-} ions. In SEM images of the all samples, gray and white regions are evident, but their amounts are different. Therefore, according to the SEM results, it can be noted that the changes in the current density, duty cycle and time could affect the formation of alumina and alumina silica phases as well as amount of them. As it discussed elsewhere [16], when the duty cycle increases, the number of microdischarges decreases. In addition, the molten aluminum eject from discharge channels. Therefore, with decreasing the number of micro-discharges, lesser amount of molten aluminum can come out and form alumina phase on the surface of the coating.

Surface porosity percent and mean pore size of the coatings are presented in figure 8 which were calculated by analyzing the figure 5 images using image j software. The graph in figure 8 indicates that both surface porosity and mean pore size of the coating decreased with increasing the current density. It has been reported [18] that when the current density increases, the number of microdischarges does not change, but the intensity of them increases. Thereby, raises the size of the coating micropores and surface

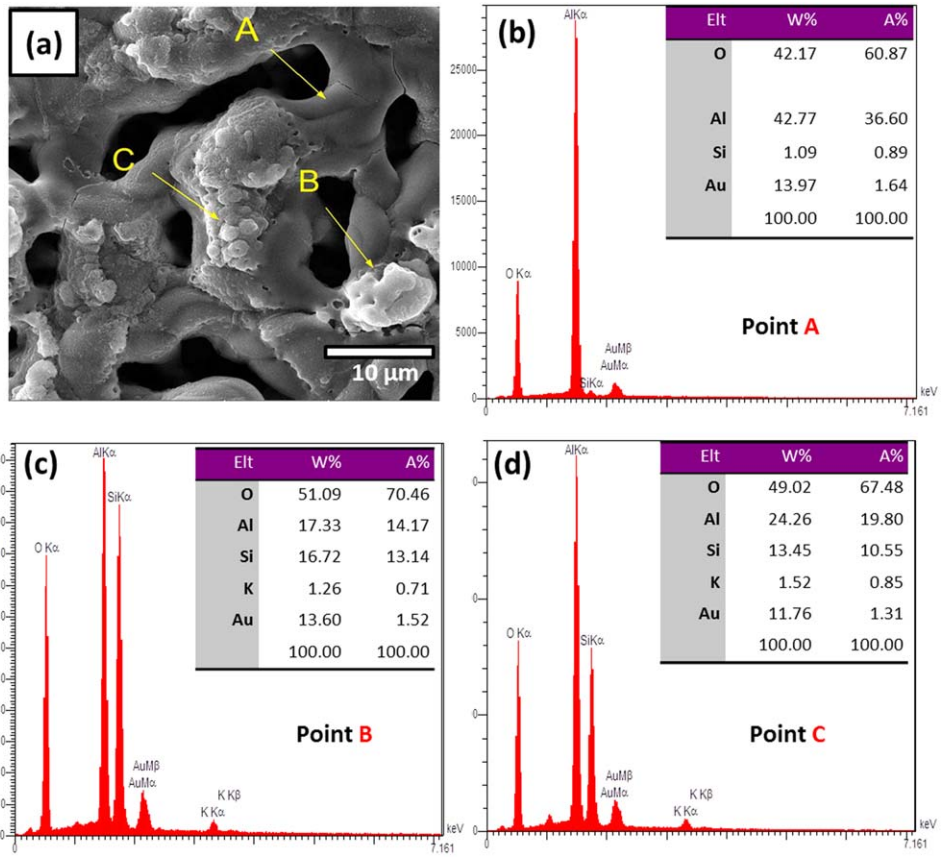

Figure 7. EDX analysis of S576 coating: (a) the SEM micrographs, (b) EDX analysis from point A, (c) EDX analysis from point B and (d) EDX analysis from point C.

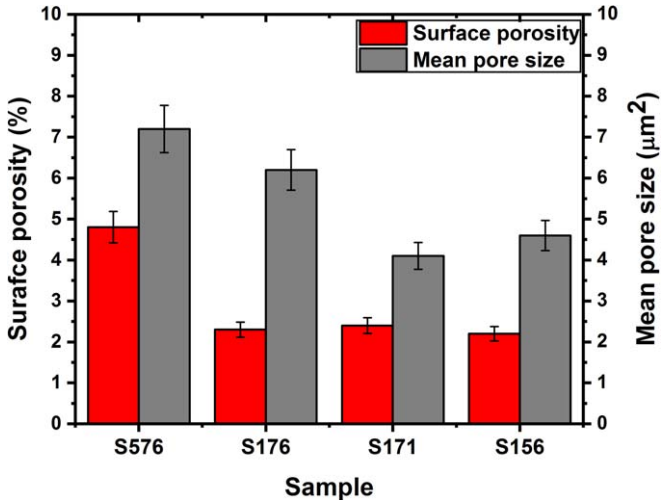

Figure 8. Results of surface porosity and mean pore size analysis by image j software.

roughness. But the results of roughness and porosity (figures 3 and 8) indicate that S176 sample has a lower roughness value than S576 sample, which may be due to a reduction of approximately twice the porosity percentage and the closure of large pores. By decreasing the duty cycle in S156 sample, the coating surface porosity decreased compared to the S176 sample. Characteristics of microdischarges have a significant effect on the size and number of the pores in plasma electrolytic oxidation coatings, because each of the discharge channels becomes a micropore in the coating after the completion of the process. As shown in figure 2, the number of microdischarges over S156 sample is more than S176 sample at the end of the coating process, but their size are smaller which confirm results of image analysis.

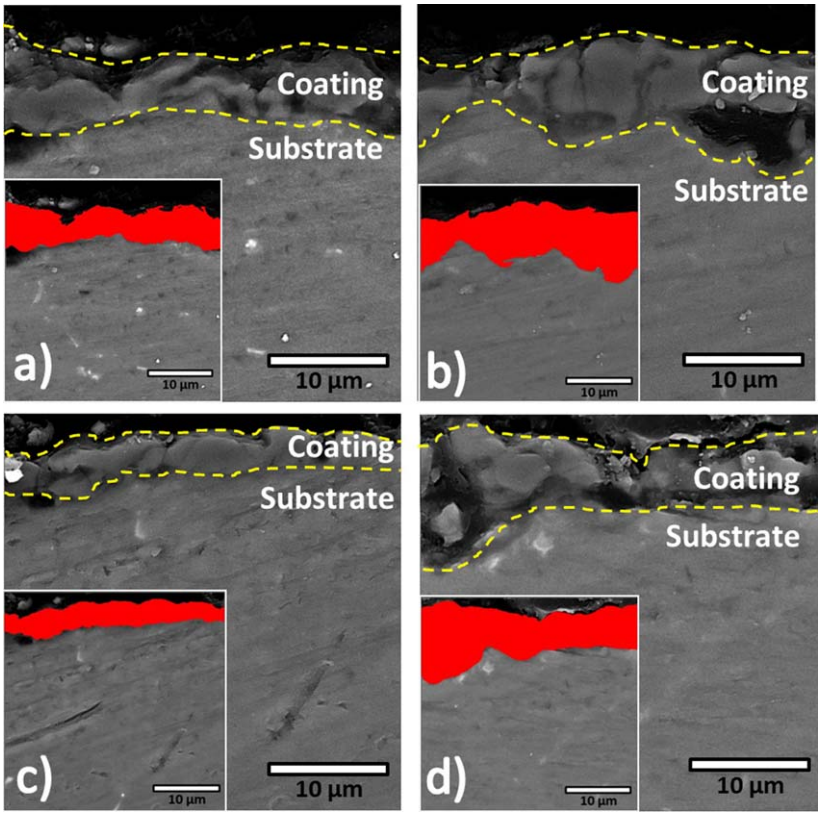

Figure 9. The SEM cross-sectional image of (a) S576, (b) S176, (c) S171 and (d) S156 samples.

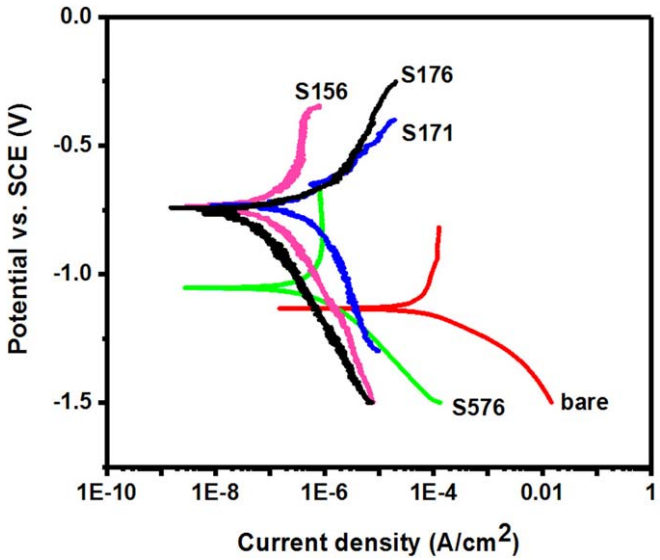

Figure 10. Potentiodynamic polarization curves of substrate and PEO coated samples.

Figure 9 shows the cross-sectional view of the coatings as well as their thickness analysis by the MIP software. The average thicknesses measured by this software for S576, S176, S156 and S171 samples are 4.9, 7.6, 7.1 and 3.3 μm, respectively; which are in consistence with the values measured by the thickness measurement gauge. Generally, all coatings possess a non-homogeneous and irregular interface with the substrate. Coating cross sections of S156 and S176 samples show that with increasing the duty cycle, a more compact coating with lesser number of micropores was achieved in S176 sample. However, the surface porosity has not changed significantly.

The potentiodynamic polarization curves of the PEO coated and bare samples in a 3.5 wt% NaCl media are shown in figure 10. Tofel Extrapolation Method were used to acquire the corrosion potential (E_{corr}), corrosion current density (i_{corr}) and anodic/cathodic

Table 2. Electrochemical data for the substrate and PEO coated samples from potentiodynamic polarization studies.

Sample	E_{corr} (V)	I_{corr} (A cm^{-2})	β_a (V)	β_c (V)	R_p ($\Omega.cm^2$)
Substrate	−1.13	5.85×10^{-5}	0.64	0.09	585.7×10^4
S576	−1.05	5.49×10^{-7}	0.31	0.19	9.317×10^4
S176	−0.75	4.17×10^{-8}	0.08	0.25	6.310×10^5
S156	−0.74	1.38×10^{-7}	0.35	0.41	5.941×10^5
S171	−0.73	4.13×10^{-7}	0.17	0.30	1.140×10^5

Tafel slopes (βa and βc). The polarization resistance (R_p) values were calculated using the stern-geary equation (equation (1)) [26]. Results extracted from the potentiodynamic polarization curves are presented in table 2.

$$R_p = \frac{\beta_a \times \beta_c}{2.303 i_{corr}(\beta_a + \beta_c)} \quad (1)$$

Corrosion current density of the PEO treated samples are decreased significantly in comparison with the bare alloy and its values was about two orders of magnitude lower than that of the substrate. Also, all the PEO treated samples had a higher corrosion potential compared to the substrate. Accordingly, both the corrosion potential increment and the corrosion current density decrement confirm that the PEO coatings had an effective corrosion protection. The coatings are like a barrier between the substrate and corrosive environment; thus it is harder for corrosive ions to pass through the dense structure of the coating and reach the substrate. Thereby, the corrosion resistance of the substrate increases. The increment of all process parameters, including current density, duty cycle and treatment time make both E_{corr} and R_p values to be increased and S176 sample showed the best corrosion resistance. Among all process parameters, the change in current density had a more considerable influence on both corrosion current density and corrosion potential. The SEM images of coatings showed that with increasing the current density, coating thickness increased and its surface and cross section porosity decreased. It has been reported that the coating defects (pores, cracks and etc.) and thickness are the most dominant factors that can affects corrosion properties of PEO coatings [18, 27, 28]. Therefore, the superior corrosion resistance of S176 sample in comparison with S576 sample is reasonable. With increasing duty cycle, corrosion potential did not change significantly, but corrosion current density decreased and led to increased polarization value in S176 sample as compared to S156 sample. This superior corrosion resistance of the S176 sample despite its almost identical thickness with S156 sample can be attributed to the compactness of the coating. It has been reported that coating thickness may not affect the corrosion resistance and a thinner coating with more compact structure could show higher corrosion resistance [29]. Although figure 8 shows that the surface porosity did not change and mean pore size increased in S176 sample, SEM images of coatings cross sections in figure 9 show that S176 coating is more compact and possess less number of pores in its structure. Comparison of polarization curves of S171 and S176 indicate that the increasing PEO processing time remarkably reduced the corrosion current density (about one order of magnitude) and increased corrosion resistance which was due to its higher thickness.

Conclusions

1. Plasma electrolytic oxidation coatings were produced on cast A356 aluminum alloy using different combination of current density, duty cycle and treatment time.
2. The Coting thickness increased with increasing current density and time, but duty cycle did not have a considerable effect, because changing the duty cycle neither influence the intensity of microdischarges, nor influence number of them.
3. Although by increasing the duty cycle, the coating thickness remained almost constant, surface roughness decreased which attributed to closure of big pores and formation of more compact structure in S176 sample.
4. All coatings were composed of gamma alumina. Current density, duty cycle and time did not have a notable effect on phases of the coatings.
5. Corrosion resistance of the coated samples improved by increasing current density, duty cycle and processing time. Sample S176 showed the best corrosion resistance with corrosion current density of 4.17×10^{-8} A.cm^{-2} and polarization resistance of 6.310×10^5 $\Omega.cm^2$ which related to its higher degree of compactness.

Acknowledgments

This research work has been supported with research grant (NO.:247383) by Materials and Energy Research Center (MERC), Karaj, Iran.

ORCID iDs

Sina Rahimi https://orcid.org/0000-0002-7497-6511

References

[1] Ye H 2003 An overview of the development of Al–Si-alloy based material for engine applications *J. Mater. Eng. Perform.* **12** 288–97

[2] Javidani M and Larouche D 2014 Application of cast Al–Si alloys in internal combustion engine components *Int. Mater. Rev.* **59** 132–58

[3] Li X *et al* 2005 Corrosion protection properties of anodic oxide coatings on an Al–Si alloy *Surf. Coat. Technol.* **200** 1994–2000

[4] He J *et al* 2009 Influence of silicon on growth process of plasma electrolytic oxidation coating on Al–Si alloy *J. Alloys Compd.* **471** 395–9

[5] Gulec A E, Gencer Y and Tarakci M 2015 The characterization of oxide based ceramic coating synthesized on Al–Si binary alloys by microarc oxidation *Surf. Coat. Technol.* **269** 100–7

[6] Mohedano M *et al* 2020 PEO coating with Ce-sealing for corrosion protection of LPSO Mg–Y–Zn alloy *Surf. Coat. Technol.* **383** 125253

[7] Rahimi S *et al* 2018 Comparison of corrosion and antibacterial properties of Al alloy treated by plasma electrolytic oxidation and anodizing methods *Mater. Today-Proc.* 5, 15667–76

[8] Ghasemi A *et al* 2010 The role of anions in the formation and corrosion resistance of the plasma electrolytic oxidation coatings *Surf. Coat. Technol.* **204** 1469–78

[9] Li Z, Yuan Y and Jing X 2014 Comparison of plasma electrolytic oxidation coatings on Mg–Li alloy formed in molybdate/silicate and aluminate/silicate composite electrolytes *Mater. Corros.* **65** 493–501

[10] Kaseem M *et al* 2015 Effect of sodium benzoate on corrosion behavior of 6061 Al alloy processed by plasma electrolytic oxidation *Surf. Coat. Technol.* **283** 268–73

[11] Wang L and Nie X 2006 Silicon effects on formation of EPO oxide coatings on aluminum alloys *Thin Solid Films* **494** 211–8

[12] Xu F, Xia Y and Li G 2009 The mechanism of PEO process on Al–Si alloys with the bulk primary silicon *Appl. Surf. Sci.* **255** 9531–8

[13] Xie H-J *et al* 2017 Wear and corrosion resistant coatings on surface of cast A356 aluminum alloy by plasma electrolytic oxidation in moderately concentrated aluminate electrolytes *Transactions of Nonferrous Metals Society of China* **27** 336–51

[14] Ikonopisov S 1977 Theory of electrical breakdown during formation of barrier anodic films *Electrochim. Acta* **22** 1077–82

[15] Al Bosta M M, Ma K-J and Chien H-H 2013 The effect of MAO processing time on surface properties and low temperature infrared emissivity of ceramic coating on aluminium 6061 alloy *Infrared Phys. Technol.* **60** 323–34

[16] Dehnavi V *et al* 2013 Effect of duty cycle and applied current frequency on plasma electrolytic oxidation (PEO) coating growth behavior *Surf. Coat. Technol.* **226** 100–7

[17] Arunnellaiappan T *et al* 2015 Influence of frequency and duty cycle on microstructure of plasma electrolytic oxidized AA7075 and the correlation to its corrosion behavior *Surf. Coat. Technol.* **280** 136–47

[18] Dehnavi V *et al* 2015 Corrosion properties of plasma electrolytic oxidation coatings on an aluminium alloy–the effect of the PEO process stage *Mater. Chem. Phys.* **161** 49–58

[19] Zhang Y *et al* 2017 Micro-structures and growth mechanisms of plasma electrolytic oxidation coatings on aluminium at different current densities *Surf. Coat. Technol.* **321** 236–46

[20] Khan R *et al* 2010 Surface characterisation of DC plasma electrolytic oxidation treated 6082 aluminium alloy: effect of current density and electrolyte concentration *Surf. Coat. Technol.* **205** 1679–88

[21] Krishna L R, Somaraju K and Sundararajan G 2003 The tribological performance of ultra-hard ceramic composite coatings obtained through microarc oxidation *Surf. Coat. Technol.* **163** 484–90

[22] Javidi M and Fadaee H 2013 Plasma electrolytic oxidation of 2024-T3 aluminum alloy and investigation on microstructure and wear behavior *Appl. Surf. Sci.* **286** 212–9

[23] Gu W-C *et al* 2007 Characterisation of ceramic coatings produced by plasma electrolytic oxidation of aluminum alloy *Mater. Sci. Eng. A* **447** 158–62

[24] Yerokhin A L, Lyubimov V V and Ashitkov R V 1998 Phase formation in ceramic coatings during plasma electrolytic oxidation of aluminium alloys *Ceram. Int.* **24** 1–6

[25] Wang P *et al* 2016 Ceramic coating formation on high Si containing Al alloy by PEO process *Surf. Eng.* **32** 428–34

[26] Stern M and Geary A 1957 A theoretical analysis of the shape of polarization curves *J. Electrochem. Soc.* **104** 56–63

[27] Prasad M S *et al* 2017 Improving the corrosion properties of magnesium AZ31 alloy GTA weld metal using microarc oxidation process *Int. J. Miner. Metall. Mater.* **24** 566–73

[28] Movahedi N and Habibolahzadeh A 2016 Effect of plasma electrolytic oxidation treatment on corrosion behavior of closed-cell Al-A356 alloy foam *Mater. Lett.* **164** 558–61

[29] Srinivasan P B *et al* 2009 Effect of current density on the microstructure and corrosion behaviour of plasma electrolytic oxidation treated AM50 magnesium alloy *Appl. Surf. Sci.* **255** 4212–8